Provisional chapter

Etching of Silicon Carbide Using Chlorine Trifluoride Gas

Hitoshi Habuka

Additional information is available at the end of the chapter

1. Introduction

Silicon carbide (SiC) is known as an excellent material. Single-crystalline 4H-silicon carbide is a fascinating wide band-gap semiconductor material [1-3], suitable for high power and high temperature electronic devices [4] because of its suitable properties, such as high electron mobility, high thermal conductivity, high chemical stability, high mechanical hardness, high break down electric field and small dielectric constant [4, 5]. Additionally, many researchers have reported the stability of silicon carbide micro-electromechanical systems (MEMS) under corrosive conditions using acid and alkaline chemical reagents [6-9]. Polycrystalline 3C-silicon carbide is widely used for various purposes, such as dummy wafers and reactor parts, in silicon semiconductor device production processes.

In the semiconductor materials production technology [10], the electronics devices manufacturing process needs an easy and cost effective technique, such as wet and/or dry cleaning, for preparing the clean surface of the substrate materials. However, the suitable properties of silicon carbide often provided difficult Problems. The chemically and mechanically stable nature often makes it very difficult to prepare the entire surface in the wafer production process, such as surface polishing and removal of any damaged layer. Useful chemical reagents and processes should be developed for silicon carbide material production.

Wet and dry etching methods of silicon carbide have been studied by many researchers [5, 11-21], using various gases and various wet etchants. However, the largest etching rate reported was nearly 1 μm/min. Here, chlorine trifluoride (ClF_3) gas is very reactive even at low temperatures and has a very strong capability to etch various materials, such as silicon [22] without plasma assistance.

In Section 2, details of polycrystalline 3C-silicon carbide etching using chlorine trifluoride gas [23, 24] are reviewed, particularly focusing on the etching rate, gaseous products, surface chemical bonds and the surface morphology of the silicon carbide. In Section 3, the dry etching of single-crystalline 4H-silicon carbide using chlorine trifluoride gas [25-29] over the wide temperature range of 570-1570 K is reviewed, particularly about the etching rate, surface chemical reaction rate constant, surface morphology and etch pits.

2. Polycrystalline 3C-Silicon Carbide Etching Using Chlorine Trifluoride Gas

2.1. Reactor and processes using chlorine trifluoride gas

In order to etch silicon carbide by chlorine trifluoride gas, the horizontal cold-wall reactor shown in Figure 1. is used. This reactor consists of a gas supply system, a quartz chamber and infrared lamps. A 30 mm wide x 40 mm long x 0.2-1 mm thick 3C-silicon carbide substrate manufactured using chemical vapor deposition (CVD) (Admap Inc., Tokyo) is held horizontally on the bottom wall of the quartz chamber.

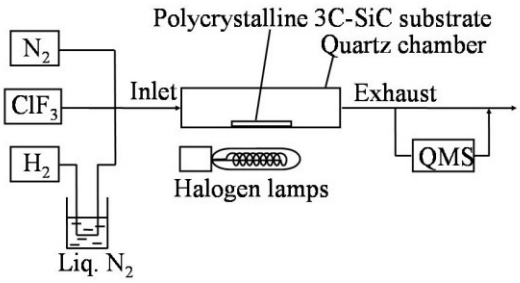

Figure 1. Horizontal cold-wall reactor used for etching polycrystalline 3C-silicon carbide substrate.

The gas supply system introduces chlorine trifluoride gas, nitrogen gas and hydrogen gas. Hydrogen gas is used to remove the silicon oxide film on the silicon carbide substrate surface, the same as those on the silicon surface [22]. The height and width of the quartz chamber are compactly designed to be 10 mm and 40 mm, respectively, similar to the chamber in our various studies [22, 30].

The etching using chlorine trifluoride gas is carried out following the process shown in Figure 2. There are mainly three steps.

(a) cleaning the silicon carbide substrate surface by baking in ambient hydrogen at 1370 K for 10 min,

(b) changing the gas from hydrogen to nitrogen, and

(c) etching the silicon carbide substrate surface using chlorine trifluoride gas.

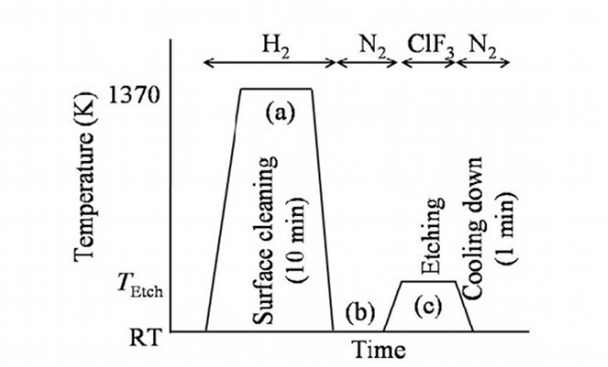

Figure 2. Process for cleaning and etching polycrystalline 3C-silicon carbide surface.

During step (a), hydrogen gas is introduced at atmospheric pressure into the reactor at a flow rate of 2 slm. Next, in step (b), the quartz chamber and the silicon carbide substrate are cooled to room temperature. The hydrogen gas present in the quartz chamber must be sufficiently purged with nitrogen gas to avoid an explosive reaction between hydrogen and chlorine trifluoride. During step (c), the silicon carbide substrate is heated and adjusted to temperatures between 670 K and 970 K. The silicon carbide substrate is etched by chlorine trifluoride (>99.9 %, Kanto Denka Kogyo Co., Ltd., Tokyo) at a flow rate of 0.1-0.25 slm without further purification and without dilution. In order to evaluate the gaseous products, part of the exhaust gas from the reactor is fed into a quadrupole mass spectra (QMS) analyzer, as shown in Figure 1. The silicon carbide etching rate using chlorine trifluoride gas is evaluated from the decrease in the weight of the silicon carbide substrate. The surface morphology of the polycrystalline 3C-silicon carbide substrate before and after the etching is observed using an optical microscope. The root-mean-square (RMS) surface roughness and the average roughness, R_a, are measured. In order to evaluate the condition of the chemical bonds of the silicon carbide surface before and after the etching, X-ray photoelectron spectra (XPS) are obtained.

2.2. Etching rate

The etching rate of the polycrystalline 3C-silicon carbide substrate surface is shown in Figure 3, which was obtained using 100% chlorine trifluoride gas at various gas flow rates in the temperature range of 670 to 970 K at atmospheric pressure. The squares, circles and triangles show the etching rate at the chlorine trifluoride gas flow rate of 0.2, 0.1 and 0.05 slm, respectively. As shown in Figure 3, the etching rate at the substrate temperature less than 670K is quite low; its value is less than 1 μm/min. However, with the increasing substrate temperature, the etching rate significantly increases particularly near 720 K. At the substrate

temperature of 770 K, the etching rate at the flow rate of 0.2 slm becomes 20 μm/min; it remains constant at substrate temperatures greater than 770 K.

As shown in Figure 3, the etching rate changes with the flow rates. The etching rates are 25, 10 and 5 μm/min at the flow rates of 0.2, 0.1 and 0.05 slm, respectively. For each chlorine trifluoride gas flow rate, the trend in the flat etching rate at temperature greater than 770K is maintained.

In order to evaluate the influence of chlorine trifluoride gas concentration, the etching rate of the polycrystalline 3C-silicon carbide substrate surface using 10-100% chlorine trifluoride gas in ambient nitrogen was measured at the flow rate of 0.2 slm, atmospheric pressure and 670-970 K, as shown in Figure 4. In this figure, the square, reverse triangle, circle, diamond, and triangle show the substrate temperatures of 670, 730, 770, 870 and 970 K, respectively. Being consistent with Figure 3, the etching rate at the substrate temperature of 670K is very low. The etching rates at 730 K are significantly higher that those at 670 K.

At the substrate temperature of 770 K, the etching rate is proportional to the chlorine trifluoride gas concentration. At 870 and 970 K, the etching rate at each chlorine trifluoride gas concentration is the same as that at 770 K. Therefore, when the substrate temperature is higher than 770 K, the etching rate over a very wide chlorine trifluoride gas concentration range is not affected by the substrate temperature.

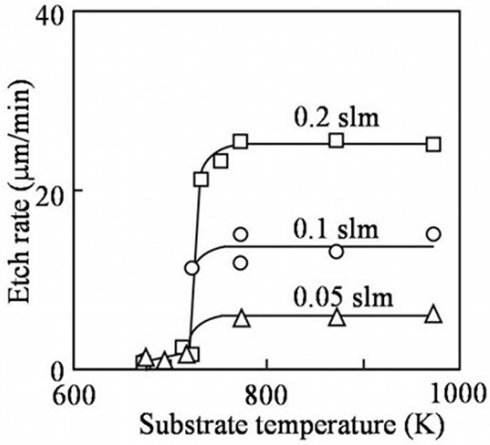

Figure 3. Etching rate of the polycrystalline 3C-silicon carbide substrate surface by chlorine trifluoride gas (100%) at atmospheric pressure in the temperature range between 670 and 970 K. Square: 0.2 slm, circle: 0.1 slm, and triangle: 0.05 slm.

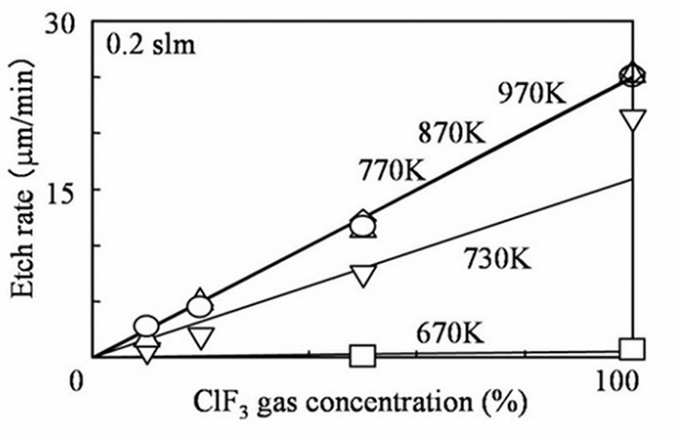

Figure 4. Etching rate of the polycrystalline 3C-silicon carbide substrate surface using chlorine trifluoride gas at 10-100%, 0.2 slm, atmospheric pressure, and 670-970K. Square: 670 K, reverse triangle: 730K, circle: 770K, diamond: 870 K, and triangle:970K.

2.3. Surface morphology and roughness

The change in the surface morphology of the 3C-silicon carbide is explained. Figure 5 shows photographs of the silicon carbide surface etched using chlorine trifluoride gas at the flow rate of 0.1 slm and atmospheric pressure at 670, 720 and 770 K for 15 min. The values in parentheses are the etch depth. Figure 5 (a) shows the initial surface which has the periodically line-shaped hills and valleys. As shown in Figure 5 (b), although the surface still has the line-shaped morphology at 670 K after 15 minutes, its pattern remains but is unclear. At the higher temperatures of 720 and 770 K, the line-shaped appearance does not remain, as shown in Figures 5 (c) and (d). In these figures, there are very small and very shallow pits having a round edge. This shows that the etching using chlorine trifluoride can smooth the large hills and valleys which existed on the silicon carbide surface.

In order to show the detail of surface smoothing effect, the change in the surface appearance is shown, in Figure 6, along etch period at a substrate temperature of 770 K and a flow rate of 0.1 slm of chlorine trifluoride. This figure shows photographs of the etched silicon carbide surface at (a) 0 min, (b) 5 min, (c) 10 min, (d) 15 min, and (e) 30 min. The values in parenthes are the etch depth. Figures 6 (a) and (d) are the same as Figures 5 (a) and (d), respectively. The relationship between the etch period and the etch depth is shown in Figure 7 (a). The line-shaped pattern in Figure 6 (a) is slightly rounded after 5 minutes. At 10 minutes, there is only a trace of the line-shaped appearance, as shown in Figure 6 (c). The 3C-silicon carbide surface has a round-shaped morphology after 15 minutes as shown in Figure 6 (d), since the line-shaped pattern is removed during the etch period between 10

and 15 minutes. The surface morphology in Figure 6 (d) is maintained at 30 minutes in Figure 6 (e), and the rounded edges of the very shallow pits do not become sharp during the last 15 minutes. Thus, the round-shaped morphology of silicon carbide surface will be maintained during etching for longer than 30 minutes.

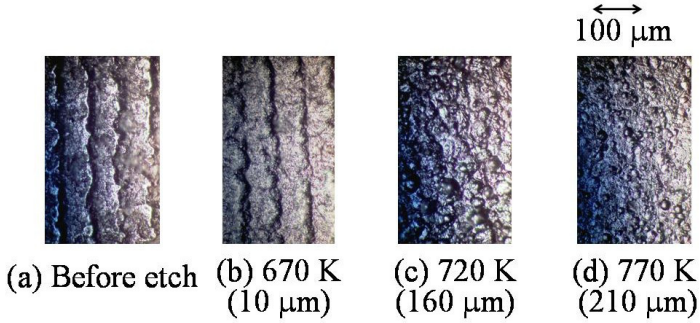

Figure 5. Photograph of the silicon carbide substrate surface etched using chlorine trifluoride at atmospheric pressure after 15 min at (b) 670 K, (c) 720 K, and (d) 770 K. (a) is the silicon carbide substrate surface before etching. The values in parentheses are the etch depth.

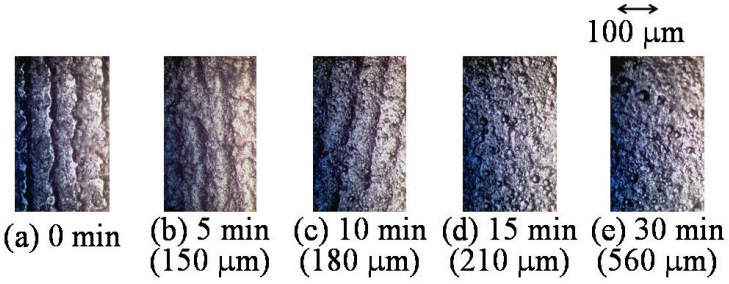

Figure 6. Photograph of the silicon carbide surface etched using chlorine trifluoride at atmospheric pressure and 770 K at (a) 0 min, (b) 5 min, (c) 10 min, (d) 15 min, and (e) 30 min. The values in parenthes are the etch depth.

In order to evaluate the surface smoothing effect of silicon carbide by chlorine trifluoride gas, the surface roughness is measured using the root-mean-square (RMS) roughness as shown in Figure 7 (b). Figure 7 (a) also shows the etch depth. The initial surface has an RMS roughness of 5 μm. The surface roughness decreases with increasing etch period. At 10 minutes, when 180 μm has been etched, the RMS roughness becomes a low value of 1 μm. Consistent with Figures 6 (d) and (e), the RMS roughness is maintained at nearly 1 μm at 30 minutes when the etch depth becomes greater than 500 μm. Solid line in Figure 7 (b) indicates the possibility that the chlorine trifluoride gas has a smoothing effect on the 3C-silicon carbide surface.

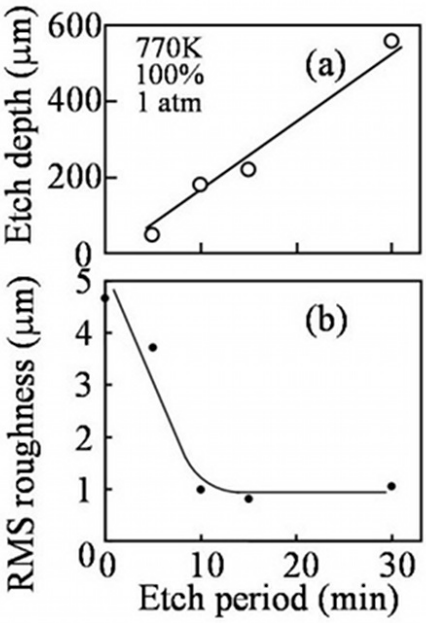

Figure 7. Etch depth and roughness of the silicon carbide surface etched by chlorine trifluoride gas at atmospheric pressure and 770 K within 30 min: (a) etch depth, and (b) root mean square (RMS) roughness.

Figure 8 shows photographs of the polycrystalline 3C-silicon carbide surface etched using a gas mixture of chlorine trifluoride and nitrogen at 670-870K for 15 min. The concentration and the flow rate of the gas mixture are 10-100% and 0.2 slm, respectively. Figure 9 shows the RMS roughness of the polycrystalline 3C-silicon carbide surface etched using chlorine trifluoride gas at atmospheric pressure and 670-870K for 15 min. The triangle, diamond and circle show the RMS roughness at the chlorine trifluoride gas concentrations of 10, 50 and 100 %, respectively.

The photograph indicated by 'Before etch' in Figure 8 shows the initial surface, which has very narrow, vague and shallow trenches formed by mechanical polishing. Using the chlorine trifluoride gas concentration of 10%, the change in the surface morphology is explained. The surface etched at 730K and 10% is recognized to have circular-shaped pits. Although the etching rate under this condition is very low, its surface shown in Figure 8 has an etched depth of 15 μm. This surface shows many circle-like pits, the edge of which is clearly shown. These may be the grain boundary or some disordered region which can be etched at a slightly higher etching rate.

At 770 K and 10 %, the shape of the circular-shaped pits still clearly exists, similar to that at 730 K and 10 %. The photograph at 870 K and 10% shows pits smaller than those at 770 K and 10%. Simultaneously, the conical shape of the pits still exists. This shows that chlorine trifluoride gas at the low concentration of 10% has a quite small role of smoothing the sur-

face, but rather tends to roughen it. This trend is measured using the RMS roughness, shown by the triangles in Figure 9. The RMS roughness before etching is nearly 0.5 μm; it increases with the increasing substrate temperature at the chlorine trifluoride gas concentration of 10%.

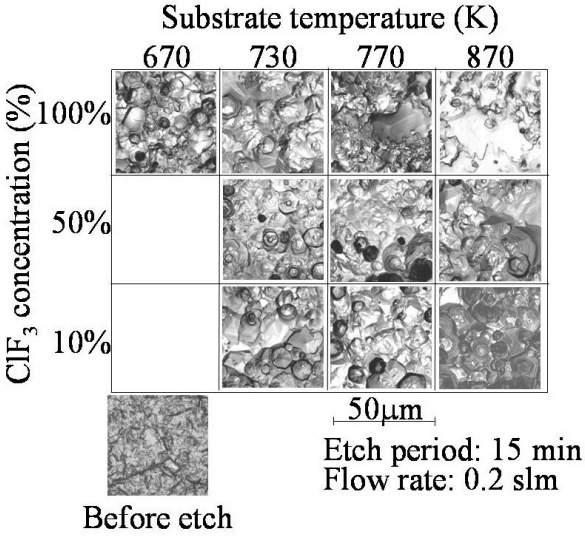

Figure 8. Photograph of the polycrystalline 3C-silicon carbide surface etched using chlorine trifluoride gas at atmospheric pressure for 15 min at 670-870 K, 10-100% and 0.2 slm.

Next, at the fixed chlorine trifluoride gas concentration of 50%, the change in the etched surface morphology is explained using Figure 8. The surface etched at 730 K and 50% shows the clear edge shape of the pits. The surface etched at 770 K and 50% still has a clear edge of the conical-shaped pits. Although some pits still have such the clearly observed edge shape, the rest of the surface has no clear edges. The surface morphology at 870 K and 50% shows both clear and vague edges. Since semi-smoothed and clear pits coexist there, the RMS roughness, indicated by the diamonds in Figure 9, still slightly increases with the increasing substrate temperature.

The change in the surface morphology etched at 100% is also shown in Figure 8. The surface etched at 670 K and 100% shows the clear edge of the pits. In contrast to this, the surface etched at 730 K and 100% shows the slightly vague edge of the pits. For the surface etched at 770 K and 100 %, the conical-shaped pits still remain, but are few. The edge of the conical-shaped pits disappears, when the surface is etched at 870 K. Since this trend in smoothing the surface appears in the RMS roughness behavior, the RMS roughness at 100%, indicated using circles in Figure 9, slightly decreases with the increasing substrate temperature.

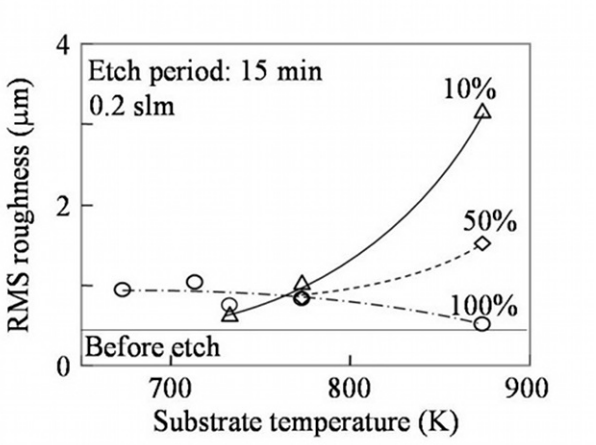

Figure 9. RMS roughness of the polycrystalline 3C-silicon carbide substrate surface etched using chlorine trifluoride gas at atmospheric pressure and 670-870 K for 15 min. Triangle: 10 %, diamond: 50 %, and circle: 100%.

From the view point of the effect of the etchant gas concentration at each temperature, the shape of the pits tends to become unclear with the increasing chlorine trifluoride gas concentration. Therefore, as the overall trend, the higher temperature and the higher chlorine trifluoride gas concentration produces a smoother surface of the polycrystalline 3C-silicon carbide.

The polycrystalline 3C-silicon carbide etching rate can be adjusted using the combination of gas flow rate, gas concentration and the substrate temperature, in order to obtain surfaces suitable for various purposes. This technique is expected to be used for various applications, such as the dry cleaning of the silicon carbide substrate surface instead of wet method, and the removal of the damaged layer formed during the chemical mechanical polishing using diamond slurry.

2.4. Surface chemical condition and etching rate

The fraction of silicon and carbon on the silicon carbide surface remaining after the etching is useful information for developing various processes which are performed after the etching. Thus, the chemical bonds at the silicon carbide surface are measured using X-ray photoelectron spectroscopy (XPS) before and after etching by chlorine trifluoride gas. Figure 10 shows the fraction of carbon, silicon, oxygen, chlorine and fluorine on the silicon carbide substrate before and after etching the depth greater than 150 μm using the chlorine trifluoride gas for 15 min at atmospheric pressure and at 720 K.

The silicon carbide surface before the etching has a carbon fraction nearly equal to that of silicon. However, the fraction of carbon significantly increases to 75 % after the etching. This indicates that the production of volatile carbon compound is slower than that of silicon compound at this temperature.

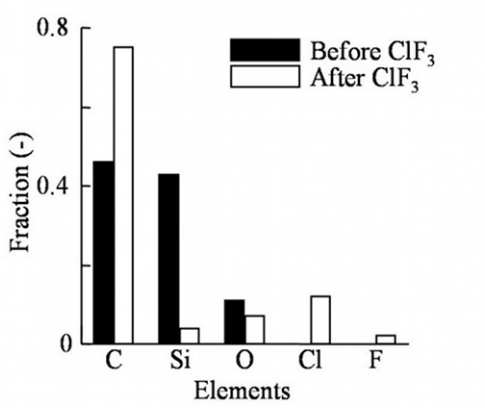

Figure 10. Fraction of carbon, silicon, oxygen, chlorine and fluorine on the silicon carbide substrate surface before and after etching using chlorine trifluoride for 15 min at atmospheric pressure in the reactor. The temperature of the silicon carbide substrate is 720 K.

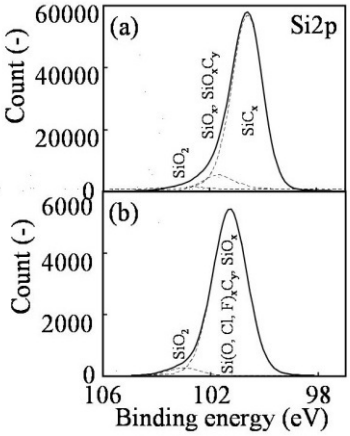

Figure 11. XPS spectra of Si 2p measured (a) before and (b) after etching using chlorine trifluoride gas for 15 min at atmospheric pressure. The temperature of the silicon carbide substrate is 720 K.

In order to evaluate the state of silicon and carbon, the XPS spectra of Si 2p and C 1s are shown in Figures 11 and 12, respectively. The conditions of etching are the same as in Figure 10.

An almost amount of silicon at the silicon carbide surface has chemical bond with carbon before etching as shown in Figure 11 (a). However, after the etching, a significant amount of silicon oxides and oxidized or halogenated silicon carbide are present as shown in Figure 11 (b). The chemical bonds of carbon simultaneously change, as same as those of silicon. Figure

12 (a) shows that chemical bonds of carbon with silicon dominate at the substrate surface before etching. After etching, an almost amount of carbon has chemical bonds with carbon as shown in Figure 12 (b). The surface after etching is covered with large amount of carbon having carbon-carbon bonds. This result is consistent with the dark appearance of the silicon carbide surface after the etching.

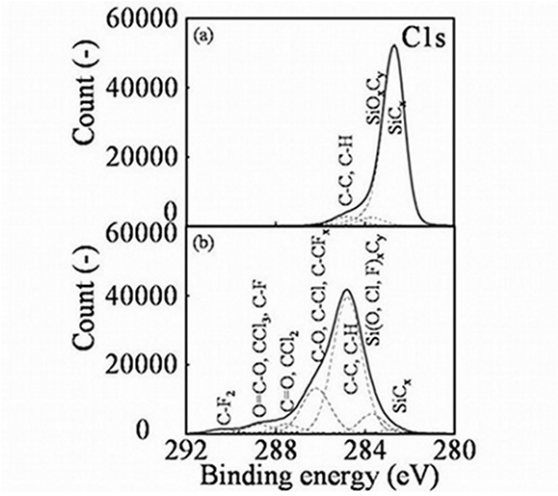

Figure 12. XPS spectra of C 1s measured (a) before and (b) after the etching using chlorine trifluoride gas for 15 min at atmospheric pressure. The temperature of the silicon carbide substrate is 720 K.

2.5. Chemical reactions

The gaseous products and the chemical reactions associated with silicon carbide etching are explained. Figure 13 shows the mass spectra of the gaseous species existing in the exhaust gas immediately after beginning silicon carbide substrate etching at 770 K using chlorine trifluoride gas at atmospheric pressure. The partial pressures are normalized using the pressure at the mass of 28 a.m.u., which is the largest partial pressure in this measurement and which can be assigned to silicon from the silicon tetrafluoride and nitrogen remaining in the QMS system.

Typical mass spectra, shown in Figure 13, are interpreted by taking into account the fragmentation in the QMS analyzer and the isotopic abundance of chlorine [31-33]. In this figure, the ion species at a mass of 14 a.m.u. is assigned to N^+, which is the fragment of nitrogen gas. The low partial pressures corresponding to chlorine trifluoride and its fragment, ClF_3^+, at masses of 92 and 94 a.m.u., and ClF^+ at 54 and 56 a.m.u., are detected. The partial pressures observed at masses of 70, 72 and 74 a.m.u. correspond to Cl_2^+, which is assigned to chlorine gas. Chlorine gas is produced due to the chemical reaction during silicon carbide

etching, similar to that for the silicon etching [22, 34]. The partial pressures at masses of 35 and 37 a.m.u. can be assigned to Cl^+, which is a fragment from both chlorine trifluoride and chlorine (Cl_2). The partial pressures observed at masses of 19 and 20 a.m.u. correspond to F^+ and HF^+, respectively. F^+ and HF^+ are produced due to the fragmentation of chlorine trifluoride. Since the partial pressure of fluorine (F_2) at mass 38 a.m.u. did not appear in the mass spectra, the thermal dissociation of chlorine trifluoride gas [35] is negligible in the gas phase of the cold wall reactor used in this study.

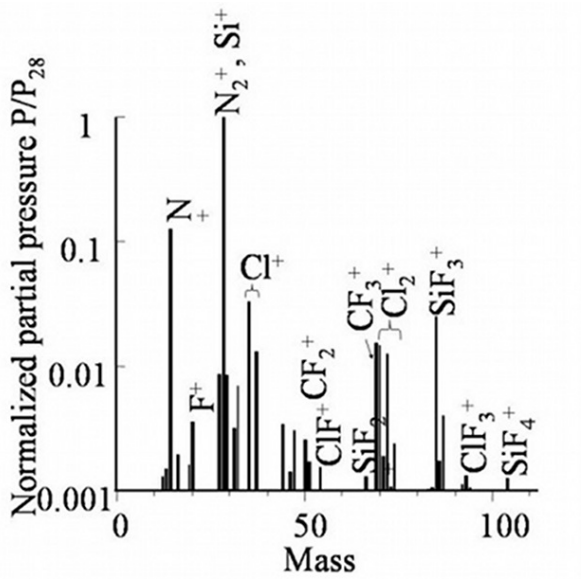

Figure 13. Mass spectra of gaseous species existing in the exhaust gas from the reactor during the etching of the silicon carbide surface using chlorine trifluoride gas at atmospheric pressure. The temperature of the silicon carbide substrate is 770 K. The ionization conditions are 70 eV and 1.73 mA.

The partial pressures at masses of 66, 85 and 104 a.m.u. can be assigned to SiF_2^+, SiF_3^+ and SiF_4^+, respectively, whose parent is silicon tetrafluoride, like silicon etching [34]. The gaseous carbon compound produced by etching is identified as carbon tetrafluoride (CF_4), because the partial pressures at masses of 50 and 69 a.m.u. correspond to CF_2^+ and CF_3^+, respectively, which can be assigned as fragments of carbon tetrafluoride.

Thus, silicon and carbon become the gaseous species of silicon tetrafluoride and carbon tetrafluoride, respectively. The overall chemical reaction between silicon carbide and chlorine trifluoride is as follows:

$$3SiC\cdot + \cdot 8ClF_3\cdot \rightarrow \cdot 3SiF_4\cdot + \cdot 3CF_4\cdot + \cdot 4Cl_2 \quad (1)$$

3. Single-Crystalline 4H-Silicon Carbide Etching Using Chlorine Trifluoride Gas

3.1. Substrate, reactor and process

The substrate used is the n-type single-crystalline 4H-silicon carbide wafer having a (0001) surface, 8-degrees off-oriented to <11-20>. This substrate has nitrogen as the n-type dopant at the concentration of 3 - 5 x 10^{18} cm^{-3}. The 4H-silicon carbide substrate, having 5 mm wide x 5 mm long x 400 μm thick dimensions, is placed on the center of the polycrystalline 3C-silicon carbide susceptor, which has the dimension of 30 mm wide × 40 mm long × 0.2 mm thick produced by the chemical vapor deposition method (Admap Inc., Tokyo).

The reactor shown in Figure 1 is used following the process shown in Figure 2 except of hydrogen baking. The Si-face (0001) and C-face (000-1) of the 4H-silicon carbide substrates are etched using chlorine trifluoride gas. The etching is performed at the temperatures between 570 – 1570 K at the chlorine trifluoride gas flow rate of 0.1 – 0.3 slm. The average etching rate of 4H-silicon carbide is determined by the decrease in the substrate weight. Because the 3C-silicon carbide susceptor and the 4H-silicon carbide substrate are simultaneously etched in the reactor, the etching rate obtained is comparable to the average value for the wide 4H-silicon carbide substrate.

The X-ray topograph of Si-face and C-face of 4H-silicon carbide was taken at the beam-line BL15C of the Photon Factory of the High Energy Accelerator Research Organization (Proposal No. 2006G286), in order to evaluate the crystalline defects. The density and behavior of etch pit produced on the 4H-silicon carbide substrate using chlorine trifluoride gas at various temperatures were evaluated.

3.2. Numerical calculation of etching rate

The etching rate of single-crystalline 4H-silicon carbide is numerically calculated [29]. The geometry of horizontal cold-wall reactor, shown in the previous section (Figure 1), is taken into account for a series of calculations. In order to evaluate the silicon carbide etching rate and the overall rate constant in steady state in non-uniformly distributed temperature and gas flow fields, the two-dimensional equations of mass, momentum, energy, species transport and surface chemical reaction, linked with the ideal gas law, are solved. The discretized equations are coupled and solved using the SIMPLE algorithm [36] on a CFD software package, Fluent version 6 (Fluent, Inc., Lebanon, NH, USA).

The silicon carbide etching is assumed to follow the overall reaction in Eq. (2) [23, 24],

$$3SiC \cdot + \cdot 8ClF_3 \cdot \rightarrow \cdot 3SiF_4 \cdot + \cdot 3CF_4 \cdot + \cdot 4Cl_2 \quad (2)$$

Mass changes due to the chemical reaction of Eq. (2) are taken into account in the boundary conditions at the surface of silicon carbide. The overall reaction shown in Eq. (2) is assumed to be a first-order reaction.

$$\text{SiC etching rate} = 6 \times 10^7 M_{SiC} k_{SiC} [ClF_3] \cdot / \cdot \rho_{SiC} \quad (\mu\text{mm min}^{-1}), \tag{3}$$

where ρ_{SiC} is the density of solid silicon carbide (kg m^{-3}). M_{SiC} is the molecular weight of silicon carbide (kg mol^{-1}), respectively. The factor 6 x 10^7 is used for the unit conversion of m s^{-1} to μm min^{-1}. k_{SiC} is the overall rate constant for the reaction of Eq. (3). [ClF_3] is the concentration of chlorine trifluoride gas at the silicon carbide surface (mol m^{-3}). The concentration of each species at the surface is governed by a balance between the consumption due to the chemical reaction and the diffusion fluxes driven by the concentration.

The gas velocity and pressure at the inlet are 0.08 m s^{-1} and 1.0133 x 10^5 Pa, respectively. The heat capacities of chlorine trifluoride, nitrogen, tetrafluorosilane, tetrafluorocarbon and chlorine are taken from the literature [37]. The gas properties, such as the viscosity and the thermal conductivity of chlorine trifluoride, tetrafluorosilane, chlorine and nitrogen are estimated with the method described in the literature [38]. The Lennard-Jones parameters of σ and ε/k for chlorine trifluoride are 4.63 Angstroms and 355 K, respectively, which are obtained using a theoretical equation [38] taking the value of viscosity [39] into account. Each physical constant is expressed as a function of temperature. The properties of the mixed gas are estimated theoretically [40]. The binary diffusion coefficients of chlorine trifluoride, tetrafluorosilane and chlorine are estimated using the method described in the literature [38].

The overall rate constant, k_{SiC} in Eq. (3) is obtained so that the calculated etching rates agree with those measured at various conditions.

3.3. Etching rate

Figure 14 shows the etching rate of the Si-face and C-face of 4H-silicon carbide at the substrate temperatures between 570 K and 1570 K. The etching rate of the C-face of 4H-silicon carbide is slightly higher than that of the Si-face of 4H-silicon carbide. The etching rate of the Si-face and C-face of 4H-silicon carbide is near 5 μm min^{-1} and it is still flat at the temperatures between 770 K and 1570 K. This flat etching rate behavior is similar to that of polycrystalline 3C-silicon carbide, shown in Figure 3 in the previous section. The various surface morphologies at higher temperatures shown in the latter part of this section are obtained at nearly the same etching rate.

Figure 15 shows the typical behavior of the etching rate changing with the chlorine trifluoride gas concentration, obtained at 1370 K. The etching rate is proportional to the chlorine trifluoride gas concentration, similar to that of polycrystalline 3C-silicon carbide, shown in Figure 4. The fluctuation of the etching rate, shown in Figures 14 and 15, is entirely 20 %, which is due to the considerable distribution of the etching rate over the 3C-silicon carbide susceptor.

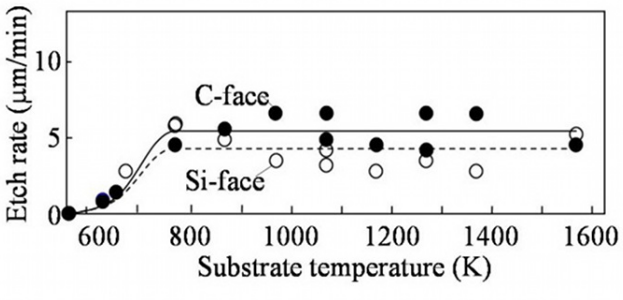

Figure 14. Etching rate of 4H-silicon carbide using chlorine trifluoride gas at 100 %, 0.1 slm and various temperatures. Dark circle: C-face, and white circle: Si-face.

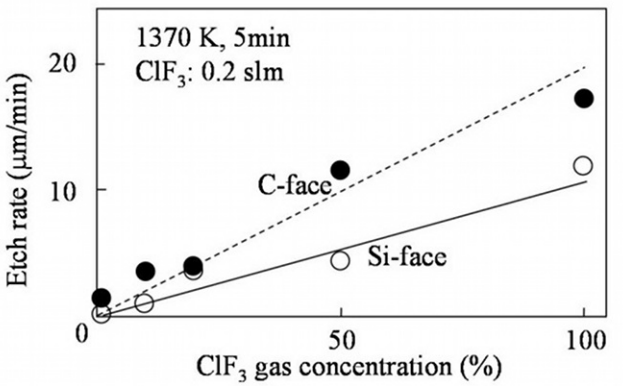

Figure 15. Etching rate of Si-face (white circle) and C-face (dark circle) 4H-silicon carbide changing with chlorine trifluoride gas concentration, at 1370 K and at the total gas flow rate of 0.2 slm for 5 min.

The relationship between the etching rate and the chlorine trifluoride gas flow rate is shown in Figures 16. Figures 16 (a) and 16 (b) show the etching rate of the Si-face and the C-face, respectively, of the 4H-silicon carbide substrate by chlorine trifluoride gas (100%) at atmospheric pressure, when changing with the chlorine trifluoride gas flow rate. The circle, square and triangle denote the etching rate at the substrate temperatures of 770, 870 and 970 K, respectively. As shown in these figures, the Si-face and C-face etching rates increase with the gas flow rate of the chlorine trifluoride gas. Additionally, the etching rate at 770, 870 and 970 K overlap each other for both the Si-face and the C-face, consistent with Figures 14. The etching rate of the Si-face is about 60 % of that of the C-face. The relationship between the Si-face etching rate and the C-face etching rate is similar to that of another empirically known etching technique, such as the potassium hydroxide method [41].

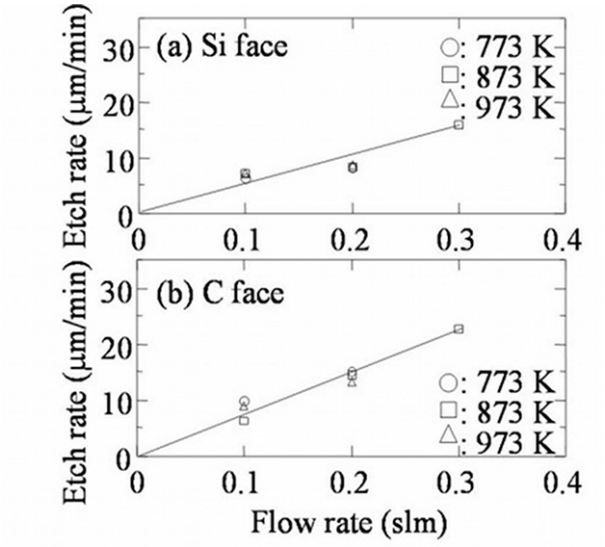

Figure 16. Etching rate of (a) Si-face and (b) C-face of 4H-silicon carbide substrate by chlorine trifluoride gas (100%) at atmospheric pressure in the flow rate range between 0.1 and 0.3 slm. Circle, square and triangle show the etching rates at the substrate temperatures of 770, 870 and 970 K, respectively.

3.4. Surface reaction rate constant

Figure 17 is the Arrhenius plot of the rate constants for etching of Si-face and C-face of 4H-silicon carbide. The rate constants is expressed in Eqs. (4) and (5).

$$k_{SiC}=4.1\ \exp\left(-6.6\ \text{x}\ 10^{4}/RT\right) \quad (\text{m/s}) \quad \text{for Si-face} \tag{4}$$

and,

$$k_{SiC}=98\ \text{x}\ \exp\left(-8.3\ \text{x}\ 10^{4}/RT\right) \quad (\text{m/s}) \quad \text{for C-face} \tag{5}$$

where R is the gas constant (J mol^{-1} K^{-1}).

In order to show that the rate constant of Eq. (4) can reproduce the measured etching rate behavior, the measured and the calculated etching rate values of Si-face are shown in Figure 18, as the Arrhenius plot. The calculation shows that the etching rate at the temperatures near 670K is near 1 μm/min, and it becomes near 10 μm/min at 1000 K. The calculated etching rate tends to become flat at the higher temperatures at the chlorine trifluoride gas flow rate of 0.1 and 0.2 slm. Additionally, the etching rate obtained by the calculation increases with increasing the chlorine trifluoride gas flow rate. Because the great etchant flow rate can moderate the etchant depletion occurring in the downstream region, the average etching

rate over the 4H-silicon carbide substrate and the 3C-silicon carbide susceptor can increase with the increasing flow rate of chlorine trifluoride gas. The etching rate for C-face calculated using Eq. (5) also showed the typical behavior of the measurement. Therefore, Eqs. (4) and (5) are applicable to reproduce the behavior of the 4H-silicon carbide (Si-face and C-face) etching rate.

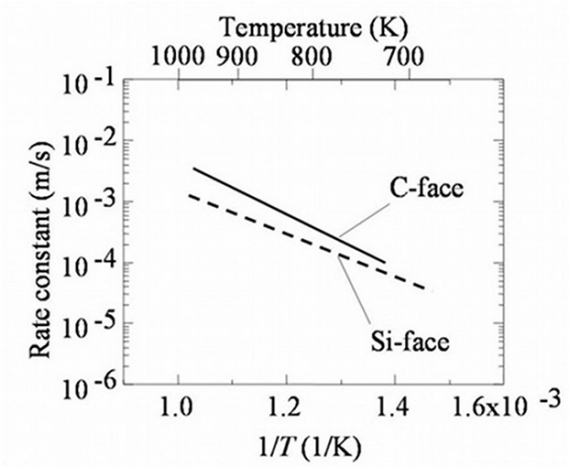

Figure 17. Rate constants for etching of Si-face (broken line) and C-face (solid line) of 4H-silicon carbide using chlorine trifluoride gas, obtained by numerical calculation.

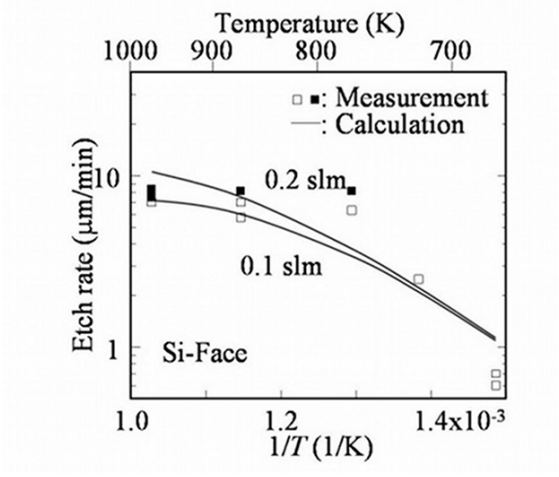

Figure 18. Arrhenius plot of 4H-silicon carbide Si-face etching rate at chlorine trifluoride flow rate of 0.1 and 0.2 slm. Square: measurement, solid line: calculation.

3.5. Surface morphology

Figure 19. shows the surface morphology of the Si-face of 4H-silicon carbide before and after the etching at the chlorine trifluoride gas concentration of 100 % and at the flow rate of 0.1 slm. The etching was performed at the substrate temperatures of (b) 570, (c) 620, (d) 770, (e) 970, (f) 1270, (g) 1370 and (h) 1570 K. The etched depth was 5-18 μm.

Figure 19 (a) shows the surface morphology of the Si-face of 4H-silicon carbide substrate before the etching. Figure 19 (b) shows that there are many small pits after the etching at 570 K. At 620 K, the pits are very large, nearly 50 μm in diameter, as shown in Figure 19 (c). With the increasing temperature, the pits tends to become small and shallow, as shown in Figures 19 (d) - (h). The pit diameter after etching at 770 K, shown in Figure 19 (d), is nearly 10 % of that at 620 K, shown in Figure 19 (c). Figure 19 (e) shows that the pit diameter becomes even smaller and the pit density decreases at 970 K. This trend is very clear at the temperatures higher than 1270 K, as shown in Figures 19 (f), (g) and (h). Figure 19 (g) shows that the pit density significantly decreases at 1370 K. The sharp-shaped pits, presented at the lower temperatures, are not there, on the silicon carbide surface after the etching at 1570 K, as shown in Figure 19 (h).

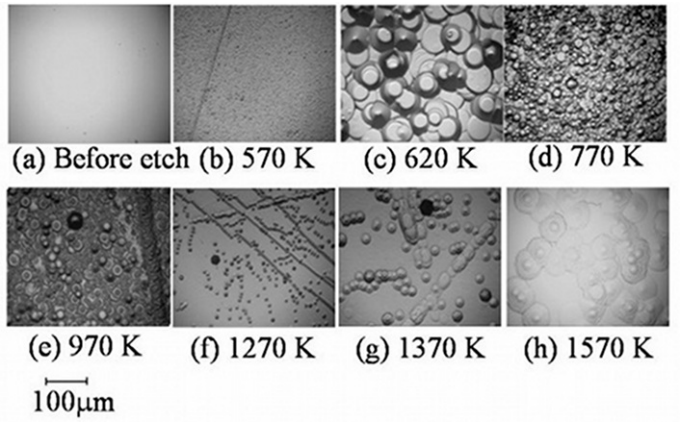

Figure 19. Surface morphology of Si-face of 4H-silicon carbide (a) before and after the etching using chlorine trifluoride gas at the concentration of 100 %, at the substrate temperature of (b) 570, (c) 620, (d) 770, (e) 970, (f) 1270, (g) 1370 and (h) 1570 K and at the flow rate of 0.1 slm. The etched depth is 5-18 μm.

Next, the influence of chlorine trifluoride gas concentration on the surface morphology is explained. Figure 20 shows the surface morphology of the Si-face 4H-silicon carbide surface taken by the optical microscope before and after the etching for 5 min at the total flow rate of 0.2 slm, at the substrate temperature of 1370 K and at various chlorine trifluoride gas concentrations. Figure 20 (a) shows the surface morphology of the Si-face of 4H-silicon carbide before the etching.

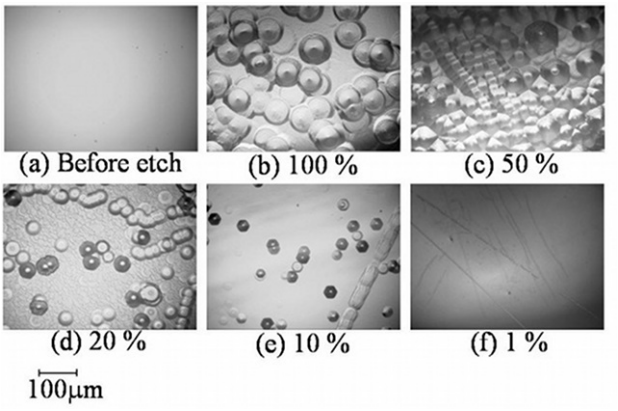

Figure 20. Surface morphology of Si-face 4H-silicon carbide surface (a) before and after etching at the total gas flow rate of 0.2 slm, 1370 K and various chlorine trifluoride gas concentrations of (b) 100, (c) 50, (d) 20, (e) 10 and (f) 1%, for 5 min.

Although there are many large pits at the chlorine trifluoride gas concentration of 100%, as shown in Figure 20 (b), they become significantly small and less at 20%, as shown in Figure 20 (d). Figure 20 (e) shows that the surface etched at 10% is flat with only a small number of pits. At 1%, most of the surface is flat, except for scratches, as shown in Figure 20 (f).

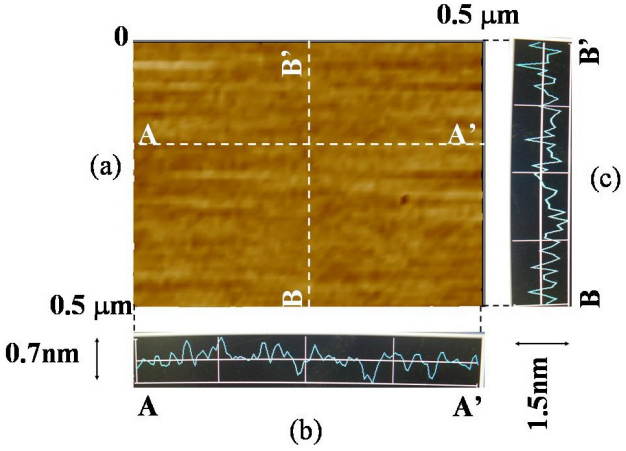

Figure 21. AFM photograph of Si-face of 4H-silicon carbide, etched for 0.5 min using the chlorine trifluoride gas concentration of 1% diluted in ambient nitrogen at the substrate temperature of 1570 K and at the total flow rate of 4 slm. (a): plan view, (b): A-A' cross section, and (c): B-B' cross section.

From Figures 19 and 20, the Si-face 4H-silicon carbide surface after etching tends to be flat with the increasing temperature and decreasing chlorine trifluoride gas concentration. Fol-

lowing this trend, the Si-face 4H-silicon carbide surface is etched at 1570 K at the chlorine trifluoride gas concentration of 1% for 0.5 min. Figure 21 shows the AFM photograph of the etched surface. Figures 21 (a), (b) and (c) are the plan view, A-A' cross section and B-B' cross section, respectively. Although the etched depth is only about 0.03 μm, it can reveal the trend of the surface, causing pit or not. As shown in Figure 21 (a), this surface does not show any etch pit; Figures 21 (b) and (c) shows no periodical shape reflecting the 4H-silicon carbide crystal step [42]. The root-mean-square (RMS) roughness are 0.1 and 0.2 nm on A-A' line and B-B' line, respectively, which are comparable to that of the polished 4H-silicon carbide substrate surface. Thus, the shallow etching for removing thin layer, such as damaged layer, is possible with maintaining the specular surface of the Si-face of 4H-silicon carbide.

Figure 22. shows the surface morphology of the C-face of 4H-silicon carbide before and after the etching at the chlorine trifluoride gas concentration of 100 %, at (b) 570, (c) 620, (d) 770, (e) 1070, (f) 1270, (g) 1370 and (h) 1570 K and at the flow rate of 0.1 slm. The etched depth is 10-30 μm. Figure 22 (a) is the C-face 4H-silicon carbide surface before the etching.

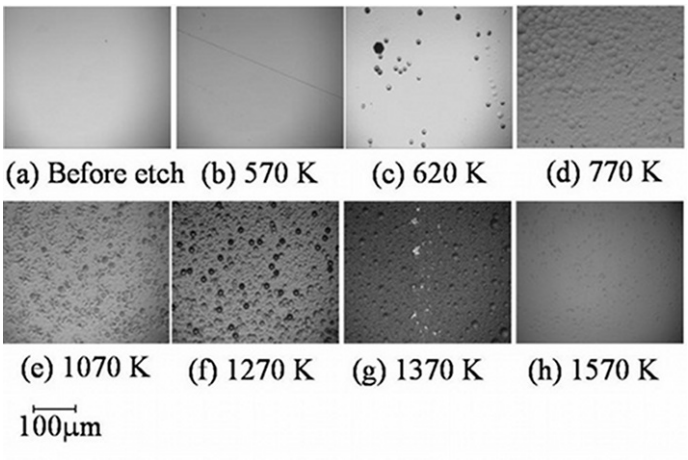

Figure 22. Surface morphology of C-face of 4H-silicon carbide (a) before and after the etching using chlorine trifluoride gas at the concentration of 100 %, at the substrate temperature of (b) 570, (c) 620, (d) 770, (e) 1070, (f) 1270, (g) 1370 and (h) 1570 K and at the flow rate of 0.1 slm. Etched depth is 10-30 μm.

There is the flat surface after the etching at 570 K, as shown in Figure 22 (b), because of significantly small etching rate. However, Figure 22 (c) shows that pits are produced at 620 K. The surface etched at the temperatures between 770 K and 1270 K have many small pits, as shown in Figures 22. (d), (e) and (f). Figures 22 (g) and (h) show that the pit diameter decreases at the temperatures higher than 1370 K. The surface etched at 1570 K shows a flat surface as shown in Figure 22 (h).

Next, the influence of the chlorine trifluoride gas concentration on the surface morphology of the C-face of 4H-silicon carbide is explained. Figure 23 shows the morphology of the C-

face 4H-silicon carbide surface before and after the etching for 5 min at the various chlorine trifluoride gas concentrations of (b) 100, (c) 50, (d) 20, (e) 10 and (f) 1% at the total flow rate of 0.2 slm. The substrate temperature is fixed at 1370 K. The etched depth is 3-84 μm.

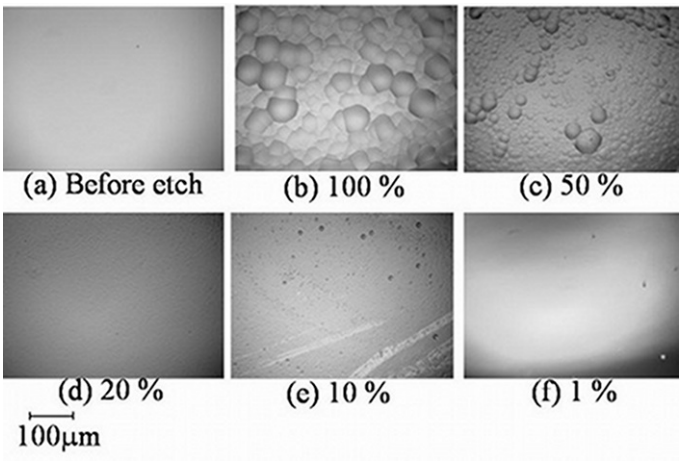

Figure 23. Surface morphology of C-face 4H-silicon carbide surface before and after etching at the total gas flow rate of 0.2 slm, 1370 K and various chlorine trifluoride gas concentrations for 5 min. (a) before etching, (b) 100, (c) 50, (d) 20, (e) 10 and (f) 1%. Etched depth is 3-84 μm.

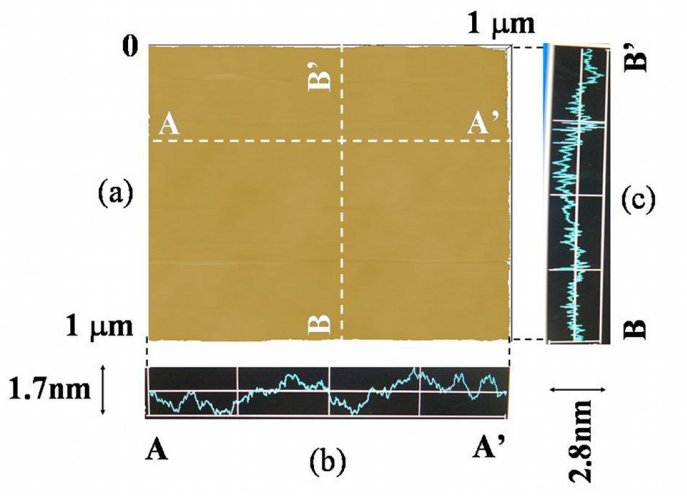

Figure 24. AFM photograph of C-face of 4H-silicon carbide, etched for 0.5 min using the chlorine trifluoride gas concentration of 1% diluted in ambient nitrogen at the substrate temperature of 1570 K and at the total flow rate of 4 slm. (a): plan view, (b): A-A' cross section, and (c): B-B' cross section.

Figure 23 (b) shows that the C-face 4H-silicon carbide surface has large and shallow pits after etching at the chlorine trifluoride gas concentration of 100%. As shown in Figure 23 (c), the etch pits become shallow at the chlorine trifluoride gas concentration of 50%. Figures 23 (d), (e) and (f) show that the etched surface is entirely flat at the chlorine trifluoride gas concentrations less than 20%. Particularly, the surface etched at 1% is flat, as shown in Figure 23 (f). Overall, the trend in the etched surface morphology of the C-face of 4H-silicon carbide is similar to that of the Si-face of 4H-silicon carbide, although the pit size of the C-face is smaller than that of Si-face.

Similar to the Si-face 4H-silicon carbide surface, the C-face 4H-silicon carbide surface is etched at 1570 K at the chlorine trifluoride gas concentration of 1% for 0.5 min. Figures 24 (a), (b) and (c) are the AFM photographs of the plan view, A-A' cross section and B-B' cross section, respectively. The etched depth is near 0.03 μm. Figure 24 (a) does not show any shape like an etch pit; Figures 24 (b) and (c) show no periodical shape reflecting the 4H-silicon carbide crystal step [42]. The RMS roughness is 0.4 and 0.3 nm on A-A’ line and B-B’ line, respectively, which are comparable to that of the polished 4H-silicon carbide substrate surface. Thus, the shallow etching without producing any trace of pit shape is possible, for the C-face of 4H-silicon carbide.

3.6. Surface morphology behavior and its rate process

Entire surface morphology behavior changing with the substrate temperature for Si-face and C-face of 4H silicon carbide is summarized as (i) very small change at very low temperatures (lower than 570 K), (ii) significant pit formation between 570 K and 1270 K, and (iii) pit formation reduced at high temperatures (higher than 1370 K).

The process of pit formation is described following the rate theory, assuming that the etch pit is formed due to the difference of the etching rate between the perfect crystal region and the weak spot having any kinds of damage and crystalline defect [10].

The rate constant of the etching in the perfect crystal region, k_{P}, is assumed to be expressed in Eq. (6).

$$k_{\mathrm{P}} = A\exp\left(-\frac{E}{RT}\right) \tag{6}$$

where A is the pre-exponential factor, E is the activation energy, R is the gas constant, and T is the substrate temperature. In contrast to this, the weak spot, which has larger etching rate to cause pit, is assumed to have the slightly smaller activation energy than that in the perfect region. The rate constant at the weak spot, k_{W}, is assumed to be expressed in Eq. (7), using the difference of the activation energy from that in the perfect region, ΔE.

$$k_{\mathrm{W}} = A\exp\left(-\frac{E-\Delta E}{RT}\right) \tag{7}$$

Assuming that the etchant gas concentration is the same in the perfect region and at the weak spot, the pit depth is expressed in Eq. (8), taking into account that $\Delta E/RT$ is very small.

$$Pit\,depth = V_{\mathrm{E}}\left(\frac{k_{\mathrm{W}}-k_{\mathrm{P}}}{k_{\mathrm{P}}}\right) = V_{\mathrm{E}}\left(\exp\left(\frac{\Delta E}{RT}\right)-1\right) \cong V_{\mathrm{E}}\frac{\Delta E}{RT} \tag{8}$$

where V_{E} is the etching rate in the perfect region.

Here, assuming that V_{E} shown in Figure 14 is the etching rate in the perfect region, the normalized pit depth, h, is evaluated and shown in Figure 25. The h value is defined using the maximum value of the pit depth, in Eq. (9).

$$h = \frac{Pit\,depth}{Pit\,depth_{\mathrm{MAX}}} = \frac{\dfrac{V_{\mathrm{E}}}{T}}{\left(\dfrac{V_{\mathrm{E},}}{T}\right)_{Pit\,depth_{\mathrm{MAX}}}} \tag{9}$$

In Figure 25, the h value at the temperatures lower than 500 K is very small; it significantly increases near 700 K. After showing its maximum, the h value gradually decreases with the increasing substrate temperature. Near 1600 K, the h value is significantly smaller than the maximum value. This trend qualitatively agrees with that of the 4H-silicon carbide surface etched using chlorine trifluoride gas. Thus, the surface morphology trend over wide temperature range can be understood mainly by the rate process.

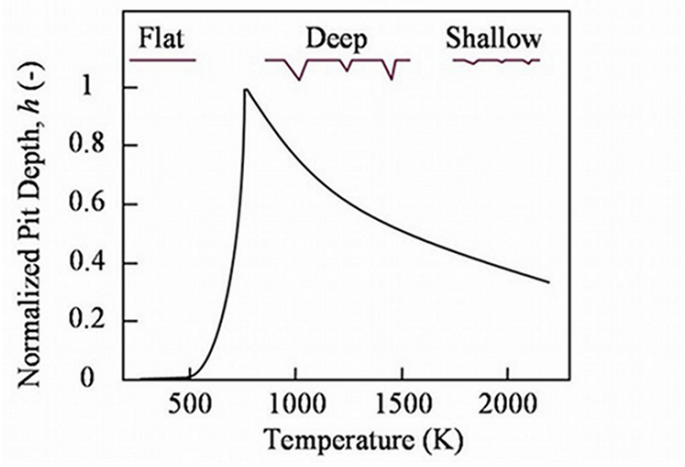

Figure 25. Normalized pit depth and temperature-dependent surface morphology behavior following the rate theory.

3.7. Etch pits and crystalline defect

AFM photographs of the pit shape formed by the chlorine trifluoride gas are shown in Figure 26. Figures 26 (a) and (b) show the pits on the Si-face and C-face, respectively, after the etching using the chlorine trifluoride gas (100%) at atmospheric pressure for 3 min at 870 K and 0.3 slm. Figure 26 (c) is the etch pit of Figure 26 (a), the edge of which is traced using dotted line.

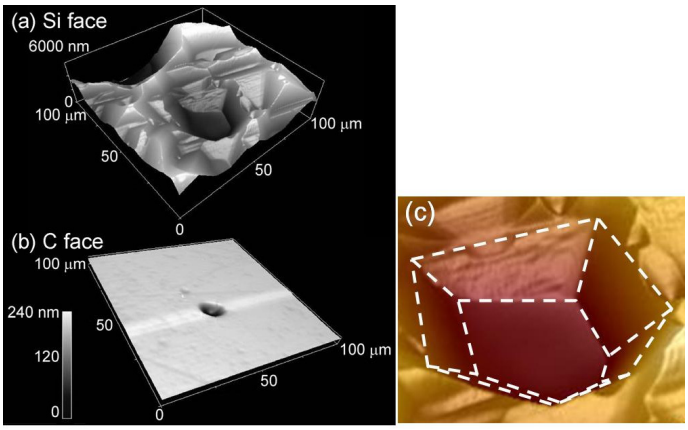

Figure 26. Etch pits on (a) Si-face and (b) C-face (870 K, chlorine trifluoride: 100 %, 0.3 slm). (c) is the magnification of the pit in (a), the edge of which is traced using dotted line.

Figures 26 (a) and (c) reveals a nearly hexagonal edge shape having a flat-shaped bottom. Its diameter and depth are about 0.03 mm and 2000-3000 nm, respectively. The many pits that exist over the entire surface are shown to have the same edge and bottom shape as that shown in Figure 26 (a). Figure 26 (b) shows the pit shape on the C-face. This surface is very flat and smooth having only a very small number of circular shaped pits, which are very shallow with a diameter of 0.01 mm and a depth of about 200 nm.

Many etch pits at the 4H-silicon carbide surface, produced by the etching using chlorine trifluoride gas, are expected to show a relationship with various crystalline defects, when the etching condition is appropriate. Thus, the Si-face and C-face 4H-silicon carbide surface are etched using chlorine trifluoride gas at 100% and at 700 K so that the pit depth become maximum value, as predicted by Figure 25. Additionally, the etch pits are compared with the X-ray topograph, because the X-ray topograph is suitable in order to evaluate an origin of etch pit [42, 43].

Figures 27 (a) and 28 (a) are the X-ray topograph of the Si-face and C-face 4H-silicon carbide surface, respectively. Figures 27 (b) and 28 (b) are the photograph of Si-face and C-face 4H-silicon carbide surface, respectively, etched using the chlorine trifluoride gas at 100% and at 700 K for 60 min. White arrows in these figures indicate the position of the spots in the X-ray topograph and the etch pits at the etched surface.

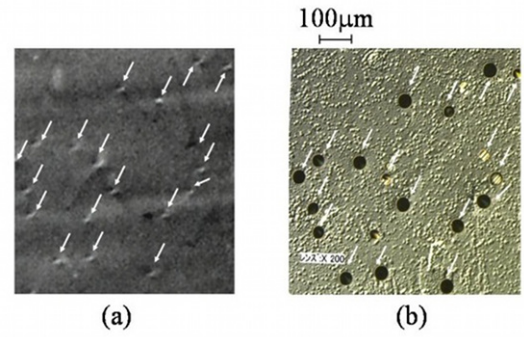

Figure 27. Comparison between the X-ray topograph and the etched Si-face 4H-silicon carbide surface. (a) X-ray topograph of the Si-face 4H silicon carbide surface, and (b) the Si-face 4H-silicon carbide surface etched using chlorine trifluoride gas at 100% and at 700 K for 60 min. Arrows in this figure indicate the spot in the X-ray topograph and the etch pit at the etched surface.

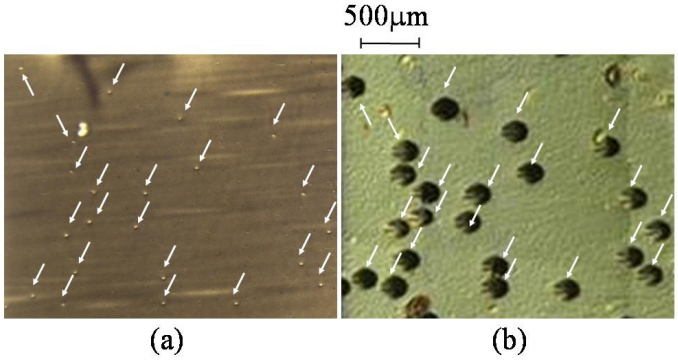

Figure 28. Comparison between the X-ray topograph and the etched C-face 4H-silicon carbide surface. (a) X-ray topograph of the Si-face 4H silicon carbide surface, and (b) the C-face 4H-silicon carbide surface etched using chlorine trifluoride gas at 100% and at 700 K for 60 min. Arrows in this figure indicate the spot in the X-ray topograph and the etch pit at the etched surface.

As indicated using white arrows, there are many etch pits, the positions of which correspond to those of the spots in the X-ray topograph. The dimension of spot in Figure 28 (a) is larger than that in Figure 27 (a); the diameter of etch pits in Figure 28 (b) is about 250 μm which is similarly larger than that in Figure 27 (b), about 40 μm. Taking into account the report [44] about the dimension of etch pits formed by KOH, Figures 28 (a) and (b) may show the screw dislocation; Figures 27 (a) and (b) may show the threading edge dislocation. Because the etching technique using the chlorine trifluoride gas may reveal the crystalline defects, like the KOH technique [44], the relationship between etch pits and various crystalline defects should be further studied.

Because of the functions to produce the specular surface and to reveal the crystalline defects, chlorine trifluoride gas is expected to be more useful than the other wet and dry techniques [41], for silicon carbide industrial process.

Next, the density and behavior of etch pit produced on the C-face of 4H-silicon carbide substrate using chlorine trifluoride gas at various temperatures were evaluated. The etch pit obtained using the chlorine trifluoride gas at 713 K for 10 min at 100% was observed and shown in Figure 29. The diameter of etch pits was near 10 μm, which was considered to be assigned to screw dislocations, following the previous study [28].

Because the etch pit density (EPD) changed with the substrate temperature [28], the etching was performed at various temperatures around 713 K. The etch pit density obtained in an area of 500 x 500 μm^2 at various substrate temperatures is shown in Figure 30. At the temperatures below 673 K, the etch pit density was very small. At 683 K, the etch pit density increase to the value near 2 x 10^4 cm^{-2}. At 713K, the etch pit density showed the maximum value of 4 x 10^4 cm^{-2}. Although the etch pit density decreased at the temperatures higher than 723 K, its value maintained near 10^4 cm^{-2}.

The etch pit density obtained at 713 K coincided with the values widely accepted as the current dislocation density level of 4H silicon carbide. Thus, the etch pit density of C-face of 4H-silicon carbide obtained in this study is acceptable and is expected to show a relationship with the crystal quality. The etch pits obtained in this study were classified to the large circular-shaped and small oval-shaped pits, which ratio were 90% and 10%, respectively, at the etching temperature of 713 K. The former is considered to be assigned to the threading screw dislocation, and the latter can be the threading edge dislocation.

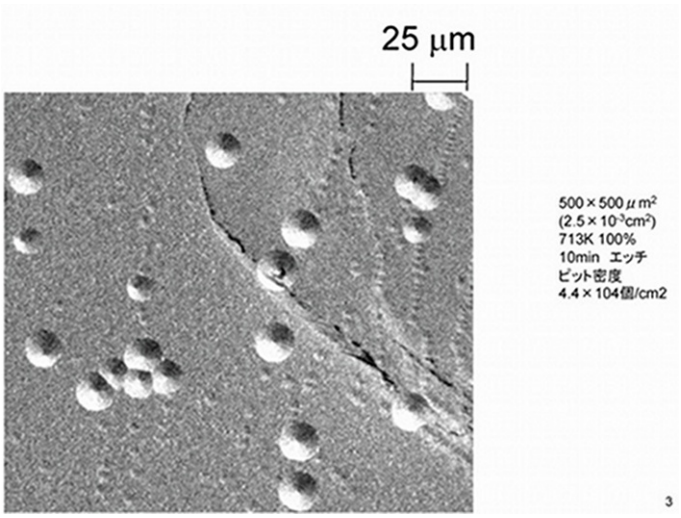

Figure 29. Etch pits produced on C-face 4H-silicon carbide surface by 100% chlorine trifluoride gas at 713 K for 10 min

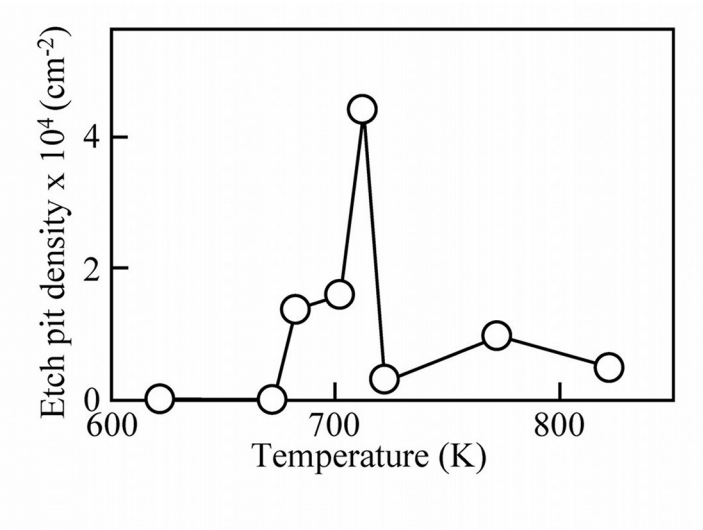

Figure 30. Etch pit density on C-face 4H-silicon carbide surface produced by chlorine trifluoride gas at various substrate temperatures.

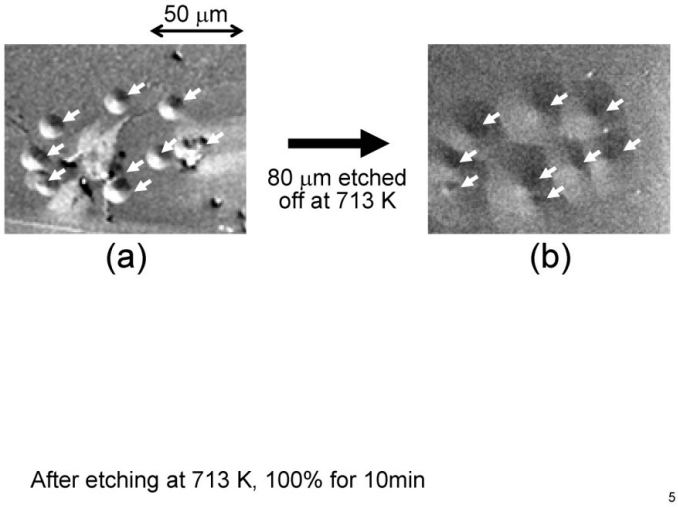

Figure 31. Comparison of etch pits (a) before and (b) after additional etching. White arrows indicate the etch pits.

In order to show that the origin of these etch pit was assigned to the crystalline imperfection, the etched surface was further etched using the same etching condition. Figure 31 (a)

shows the nine etch pits observed on the C-face of 4H silicon carbide after the etching at 713 K for 10 min using the 100 % chlorine trifluoride gas. Their diameter was about 10 – 15 μm. This substrate was additionally etched at 713 K at the 100 % chlorine trifluoride gas. Figure 31 (b) shows the surface, 80 μm of which surface was etched off by the additional etching. Figure 31 (b) shows the large and shallow nine etch pits, which were overlapped with each other. The number and the position of etch pit center in Figure. 31 (b) corresponded to those in Figure 31 (a), respectively. Thus, over the depth of 80 μm, the origin to cause the etch pit was concluded to exist; the origin could be the dislocation, such as the threading dislocation, existing normal to the substrate surface.

The results obtained in this study indicate that the pits caused by the etching using chlorine trifluoride gas at around 713 K has the origin of crystalline imperfection, such as the threading dislocation. However, the interpretation of etch pits with respect to the underlying dislocation type should be further carefully performed by a comparative investigation [28]. Additionally, the density and shape of etch pit by this technique should be further clarified and verified through many characterization.

4. Summary

Silicon carbide etching using chlorine trifluoride gas with high etching rate occurs at the temperatures higher than 770 K. Its chemical reaction is as follows:
$3SiC\cdot + \cdot 8ClF_3\cdot \rightarrow \cdot 3SiF_4\cdot + \cdot 3CF_4\cdot + \cdot 4Cl_2$

The etching rate is 10-20 μm/min and 5 μm/min, for polycrystalline 3C-silicon carbide and single-crystalline 4H-silicon carbide, respectively. The etching rate of Si-face of 4H-silicon carbide is slightly smaller than that of C-face. The etched surface tends to be carbon rich. The etched surface of Si-face of 4H-silicon carbide shows various kinds of morphology: pitted at low temperatures of 570 – 1270 K, and smooth at 1570 K. The C-face of 4H-silicon carbide shows the similar trend, and is entirely very smoother than that of Si-face. Most of the etch pits formed near 700 K at the Si-face and C-face of 4H-silicon carbide show relationship between dislocations revealed by the X-ray topograph. At the substrate temperature of 713 K, the etch pit density showed the maximum value of 4×10^4 cm^{-2}. The etch pit density obtained by this technique is considered to show the crystal quality, particularly, the dislocation density.

Acknowledgements

Various studies reviewed in this Chapter were performed with Ms. Satoko Oda, Mr. Yusuke Katsumi, Mr. Yu Kasahara, Ms. Keiko Tanaka, Mr. Kazuchika Furukawa, Mr. Yusuke Fukumoto, Dr. Yutaka Miura, Mr. Yoichi Negishi, Dr. Takashi Takeuchi, Prof. Masahiko Aihara, Prof. Minoru Takeda, Prof. Hironobu Kunieda and Prof. Kenji Aramaki of Yokohama National University, Mr. Yasushi Fukai, Mr. Katsuya Fukae, Mr. Naoto Takechi, Dr. Yuan Gao,

and Mr. Shinji Iizuka of Kanto Denka Kogyo Co., Ltd., and Dr. Tomohisa Kato, Dr. Hajime Okumura and Dr. Kazuo Arai of National Institutes of Advanced Science and Technology. Mr. N. Okumura of Keyence Co., Ltd., is very much appreciated for the surface roughness evaluation. X-ray topography experiment has been performed under the approval of the Photon Factory Program Advisory Committee (Proposal No. 2006G286).

Author details

Hitoshi Habuka*

Address all correspondence to: habuka1@ynu.ac.jp

Department of Chemical and Energy Engineering, Yokohama National University, Japan

References

[1] Gogotsi, Y., Welz, S., Ersoy, D. A., & Mc Nallan, M. J. (2001). *Nature*, 411(6835), 283.

[2] Vyshnyakova, K., Yushin, G., Pereselentseva, L., & Gogotsi, Y. (2006). *Int. J. Appl. Ceramic Tech.*, 3, 485.

[3] Zinovev, A. V., Moore, J. F., Hryn, J., & Pellin, M. J. (2006). *Surf. Sci*, 600, 2242.

[4] Cooke, M. (2005, Dec). *III-Vs Review*, 18, 40.

[5] Chai, C., Yang, Y., Li, Y., & Jia, H. (2003). *Optical Materials*, 23, 103.

[6] Mehregany, M., Zorman, C. A., Roy, S., Fleischman, A. J., Wu, C. H., & Rajan, N. (2000). *International Materials Reviews*, 45, 85.

[7] Stoldt, C. R., Carraro, C., Ashurst, W. R., Gao, D., Howe, R. T., & Maboudian, R. (2002). *Sensors and Actuators a-Physical*, 97-98, 410.

[8] Rajan, N., Mehregany, M., Zorman, C. A., Stefanescu, S., & Kicher, T. P. (1999). *Journal of Microelectromechanical Systems*, 8, 251.

[9] Ashurst, W. R., Wijesundara, M. B. J., Carraro, C., & Maboudian, R. (2004). *Tribology Letters*, 17, 195.

[10] Shimura, F. (1989). Semiconductor Silicon Crystal Technology. 244, Academic Press, San Diego, USA.

[11] Kim, B., Kim, S., Ann, S., & Lee, B. (2003). *Thin Solid Film*, 434, 276.

[12] Schmid, U., Eickoff, M., Richter, C., Kroetz, G., & Schmitt-Landsiedel, D. (2001). *Sensors and Actuators A*, 94, 87.

[13] Wolf, R., & Helbig, R. (1996). *J. Electrochem. Soc.*, 143, 1037.

[14] Yih, P. H., & Steckl, A. J. (1995). J. Electrochem. Soc., ., 142, 312.

[15] Xie, Z. Y., Wei, C. H., Li, L. Y., Yu, Q. M., & Edgar, J. H. (2000). *J. Cryst. Growth*, 217, 115.

[16] Sanchez, E. K., Ha, S., Grim, J., Skowronski, M., Vetter, W. M., Dudley, M., Bertke, R., & Mitchel, W. C. (2002). *J. Electrochem. Soc*, 149, G 131.

[17] Syvajarvi, M., Yakimova, R., & Janzen, E. (2000). *J. Electrochem. Soc*, 147, 3519.

[18] Shor, J. S., Zhang, X. G., & Osgood, R. M. (1992). *J. Electrochem. Soc*, 139, 1213.

[19] Chabert, P. (2001). *J. Vac. Sci. Technol. B*,, 19, 1339.

[20] Khan, P. A., Roof, B., Zhou, L., & Asesida, I. (2001). *J. Electron. Mater.*, 30, 212.

[21] Jiang, L., Cheung, R., Brown, R., & Mount, A. (2003). *J. Appl. Phys.*, 93, 1376.

[22] Habuka, H., Koda, H., Saito, D., Suzuki, T., Nakamura, A., Takeuchi, T., & Aihara, M. (2003). *J. Electrochem. Soc.*, 150, G461-464.

[23] Habuka, H., Oda, S., Fukai, Y., Fukae, K., Sekiguchi, T., Takeuchi, T., & Aihara, M. (2005). *Jpn. J. Appl. Phys*, 44, 1376.

[24] Habuka, H., Oda, S., Fukai, Y., Fukae, K., Takeuchi, T., & Aihara, M. (2006). *Thin Solid Films*, 514, 193.

[25] Miura, Y., Katsumi, Y., Oda, S., Habuka, H., Fukai, Y., Fukae, K., Kato, T., Okumura, H., & Arai, K. (2007). *Jpn. J. Appl. Phys*,, 46, 7875.

[26] Habuka, H., Katsumi, Y., Miura, Y., Tanaka, K., Fukai, Y., Fukae, T., Gao, Y., Kato, T., Okumura, H., & Arai, K. (2008). *Materials Science Forum*,, 600-603, 655.

[27] Habuka, H., Tanaka, K., Katsumi, Y., Takechi, N., Fukae, K., & Kato, T. (2010). *Materials Science Forum*, 645-648, 787.

[28] Habuka, H., Tanaka, K., Katsumi, Y., Takechi, N., Fukae, K., & Kato, T. (2009). *J. Electrochem. Soc*,, 156, H971.

[29] Miura, Y., Kasahara, Y., Habuka, H., Takechi, N., & Fukae, K. (2009). *Jpn. J. Appl. Phys.*, 48, 026504.

[30] Chinone, Y., Esaki, S., & Fujita, F. (1996). *Shirikon no Kagaku*, Realize,, Tokyo, 890.

[31] Habuka, H., Sukenobu, T., Koda, H., Takeuchi, T., & Aihara, M. (2004). *J. Electrochem. Soc.*, 151, G783-787.

[32] Lide, D. R., & Frederikes, H. P. R. (1997). CRC Handbook of Chemistry and Physics. , ed., D. R. Lide (CRC Press, Boca Raton, FL, 78 th ed. , 1.

[33] Lee, T. E. (1998). A Beginner's Guide to Mass Spectral Interpretation. (Wiley, Chichester, 1998).

[34] Chapman, J. R. (1993). Practical Organic Mass Spectrometry. Wiley,, Chichester.

[35] Habuka, H., Otsuka, T., Qu, W. F., & Jpn, . (1999). *J. Appl. Phys.*, 38, 6466.

[36] Saito, Y., Hirabaru, M., & Yoshida, A. (1992). *J. Vac. Sci. Technol B*,, 10, 175.

[37] Patankar, S. V. (1980). Numerical Heat Transfer and Fluid Flow. ,McGraw-Hill, New York, USA

[38] Webbook. http://webbook.nist.gov/chemistry.

[39] Reid, R. C., Prausnitz, J. M., & Poling, B. E. (1987). The Properties of Gases and Liquids. McGraw-Hill, New York 4 $_{th}$

[40] Gakujutsushinkokai, Nihon. , (1997). Fussokagaku Nyumon, Nikan Kogyo ShinbunshaTokyo, Japan [in Japanese], 86.

[41] Fluent (2001). FLUENT User's ManualVer. 5.5 (Fluent, Inc., Hanover, 2001)

[42] Matsunami, H. (2003). *Technology of Semiconductor SiC and Its Application*, Nikkan Kogyo, Tokyo, Japan.

[43] Ohno, T., Yamaguchi, H., Kuroda, S., Kojima, K., Suzuki, T., & Arai, K. (2004). *J. Cryst. Growth*, 260, 209.

[44] Ma, X., Dudley, M., Vetter, W., & Sudarshan, T. (2003). *Jpn. J. Appl. Phys.*,, 42, L1077.

[45] Takanashi, J., Kanaya, M., & Fujiwara, Y. (1994). *J. Cryst. Growth*, 135, 61.